Reconfigurable metasurfaces towards commercial success

Tian Gu[1,2,*], Hyun Jung Kim[3,4,*], Clara Rivero-Baleine[5,*], and Juejun Hu[1,2,*]

[1]*Department of Materials Science & Engineering, Massachusetts Institute of Technology, Cambridge, Massachusetts, USA*
[2]*Materials Research Laboratory, Massachusetts Institute of Technology, Cambridge, Massachusetts, USA*
[3]*National Institute of Aerospace, Hampton, Virginia, USA*
[4]*NASA Langley Research Center, Hampton, Virginia, USA*
[5]*Missiles and Fire Control, Lockheed Martin Corporation, Orlando, Florida, USA*

*****gutian@mit.edu, hyunjung.kim@nasa.gov, clara.rivero-baleine@lmco.com, hujuejun@mit.edu

Abstract

Reconfigurable optical metasurfaces are rapidly emerging as a major frontier in photonics research, development, and commercialization. They promise compact, light-weight, and energy-efficient reconfigurable optical systems with unprecedented performance and functions that can be dynamically defined on-demand. Compared to their passive counterparts, the reconfiguration capacity also set additional challenges in scalable control, manufacturing, and control toward their practical deployment. This review aims to survey the state-of-the-art of reconfigurable metasurface technologies and their applications using spaceborne remote sensing, active beam steering and light field display as examples, while highlighting key research advances essential to enabling their transition from laboratory curiosity to commercial reality.

Main

Optical metasurfaces are artificial media comprising planar arrays of sub-wavelength structures commonly called meta-atoms. With their now well-recognized advantages in optical performances, form factor and cost, metasurfaces are witnessing a move toward commercial adoption: a solid line-up of large corporations as well as a cohort of aspiring start-up companies are heavily investing on R&D in this field.

Reconfigurable metasurfaces, often alternatively termed active metasurfaces, introduce a new dimension to the space. They enable dynamic tuning of optical functions and thereby promise wide-ranging applications in analog computing[1], data communications[2], optical camouflage[3], reconfigurable imaging[4], light detection and ranging (LiDAR)[5], display[6], imaging spectroscopy[7], nonreciprocal photonics[8], and many others. As the interest in reconfigurable metasurfaces percolates from academia to industry, important questions arise regarding when and how their transition from lab to market will flourish. To address such questions, this article provides a bird's eye view on current state-of-the-art of active optical metasurface technologies. Emerging applications capitalizing on their unique attributes are subsequently surveyed. Finally, we spotlight new research frontiers that add to their functionalities and scrutinize the technological gaps that need to be filled to transform the prospective applications into reality.

The state-of-the-art in reconfigurable metasurface technologies

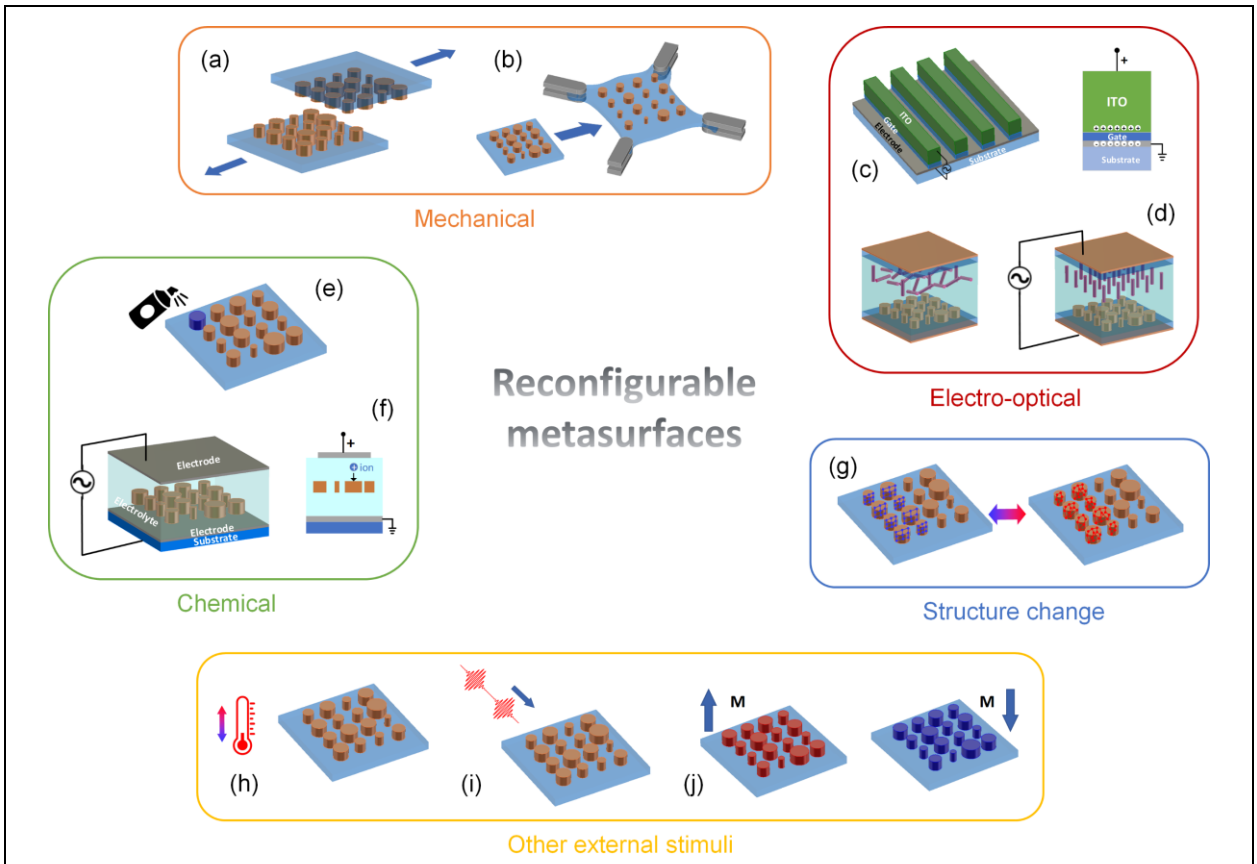

Fig. 1. Mechanisms for active tuning of reconfigurable metasurface. (a) Mechanical displacement. (b) Substrate stretching. (c) Carrier injection via gating. (d) Electro-refractive materials. (e) Chemical reaction. (f) Electrochemical ion transport. (g) Structural transition in materials. (h) Thermo-optic effect. (i) All-optical nonlinearity. (j) Magneto-optical interaction, where M denotes external magnetic field.

Active tuning schemes of metasurfaces can be classified into two categories, one where the optical responses of the meta-atoms are modified and the other relying on mechanical movement of meta-atoms. The former scheme usually involves modulating the optical properties of the meta-atoms or their surrounding material, for instance via free carrier injection[9], Pockels effect[10], quantum confined Stark effect[11], thermo-optic coupling[12], electrochromism[13], magneto-optical interaction[14], and structural transitions in various materials[15–18], whereas the latter can leverage either macroscopic displacement[19]/deformation[20] or micro-electromechanical system (MEMS) actuation[21] (Fig. 1). State-of-the-art performances of these tuning mechanisms are summarized in Table 1, and we refer the readers to other reviews on this topic for more detailed discussions[22–24].

Besides key performance attributes defined by optical contrast, loss, speed, and endurance, the likelihood of a reconfigurable metasurface technology to enter mainstream adoption in the near- or mid-term is largely dictated by its technology and manufacturing readiness levels (TRL and MRL). From this technology maturity perspective, liquid crystal (LC) and MEMS based metasurfaces are among the most established candidates. Both technologies make use of proven industry-standard technologies to introduce active tuning capabilities and can also take advantage of an established industrial ecosystem to facilitate high-volume device manufacturing and packaging. Other promising contenders involve new materials such as transparent conducting oxides (TCOs) and chalcogenide phase change materials (PCMs). Even though these materials are not part of the standard offerings of most silicon foundries today, they are amenable to foundry-compatible backend integration. TCOs constitute an integral element of modern-day display panel production process and PCMs have already become a key ingredient in commercial nonvolatile memories. Integration of these new materials and metasurface architectures into mainstream manufacturing processes will be motivated by practical application demands as discussed in the succeeding section.

Application prospects for reconfigurable metasurfaces

Before delving into the applications of reconfigurable metasurfaces, one should be reminded that actively tunable optics is not a new concept. For example, astronomical telescopes have long harnessed deformable mirror based adaptive optics for real-time wavefront correction. Spatial light modulators (SLMs) building on digital light processing or liquid crystal on silicon (LCoS) have been meticulously perfected over the past decades. So, what do reconfigurable metasurfaces have to offer?

Their small Size, Weight and Power (SWaP) metrics promise reconfigurable optical systems that are ultracompact, light-weight, energy-efficient and rugged. Their optically-thin, pixelated device architecture further enables fast tuning mechanisms not compatible with conventional bulk optics. Space applications represents an emerging arena where these characteristics are highly prized (Case Study 1). Moreover, such size down-scaling does not come with the usual penalties of compromised optical quality or lack of fine control, thereby setting reconfigurable metasurfaces apart from other competing tunable micro-optics technologies relying on electrowetting, liquid metals, and soft elastomeric optics. Reconfigurable metasurfaces are thus also well poised for applications such as augmented/virtual reality (AR/VR) and point-of-care or minimally invasive medical imaging, where form factor and optical precision are equally critical.

Another defining character of reconfigurable metasurfaces is their capacity for on-demand wavefront manipulation down to the sub-wavelength scale. This unprecedented granularity permits light bending at extreme angles that traditional refractive or diffractive optics cannot accommodate while effectively suppressing spurious diffraction orders[25–27]. Beam steering devices with high efficiency and large field-of-view (FOV) can be created capitalizing on this feature (Case

Study 2). The wide-angle beam steering capability, coupled with high spatial density afforded by metasurface optics, envisions glasses-free 3-D displays offering high resolution, large FOV, and full color coverage (Case Study 3). Finally, the ability to engineer a metasurface's phase profile in an almost arbitrary manner proves valuable to computational imaging, since the transfer function of the frontend meta-optics can be co-designed holistically with the backend processing algorithm to maximize the signal-to-noise ratio[28]. It has been shown that reconfigurable meta-optics designed using such an approach can yield *optimal* imaging systems capable of multi-dimensional (spatial, spectral, polarization, light field, etc.) information retrieval[29].

Finally, since many reconfigurable metasurfaces are produced using semiconductor nanofabrication technologies, they can be seamlessly integrated with semiconductor electronic and photonic devices to create 'metasurface-augmented' optoelectronics with novel functionalities, whereas such wafer-level integration is often challenging or impractical for conventional tunable micro-optics.

These unique advantages presented by reconfigurable metasurfaces foreshadow an array of potential applications outlined in Table 2. The key takeaway message is that there is no "one-size-fits-all" solution, because each application prioritizes a different set of performance metrics that none of the reconfigurable metasurface technologies today (Table 1) can simultaneously meet. Table 2 also distinguishes two types of tuning schemes: discrete and continuous. In the former case, the metasurface only accesses a small number of optical states, and such discrete tuning over multiple arbitrary phase profiles can be accomplished by collective switching of all meta-atoms across the aperture[30]. On the other hand, it is generally believed that continuous tuning, where a large number or a continuum of states are mandated, necessitates independent control of individual or small groups of meta-atoms. In a later section, we will propose a new concept defying this conventional wisdom to achieve continuous tuning with a much simplified switching fabric. Other research challenges that need to be addressed to fulfil the application demands will also be elaborated.

- *Case Study 1: reconfigurable metasurfaces in aerospace applications*

The growth in aerospace systems has been underpinned by increasing capabilities being packed into smaller and lighter spacecrafts, which requires robust components to deliver enhanced science data products while constrained by lean SWaP budgets. Reconfigurable metasurface optics will be game changers for aerospace remote sensing applications including:

- ✓ beam shaping for antennae (optical and microwave wavelengths);
- ✓ real-time phase-corrective lenses and planar adaptive optics for imaging, optical communications, and high-gain antennae;
- ✓ beam steering for radar and LiDAR scanning systems, flat panels, and mobile communication antennae (optical, microwaves and millimetre-wave wavelengths); and
- ✓ tunable filter and spatial light modulators for imaging spectroscopy.

As an example, exoplanet imaging by space telescopes requires real-time wavefront corrections to mitigate the effects of thermal gradients, optical imperfections, and diffraction. Reconfigurable metasurface optics could lead to a space-based correction system with major SWaP advantages, permitting characterization of light from exoplanets via active cancelation of high frequency spatial and temporal aberrations.

Another application that reconfigurable metasurfaces are poised to transform is multispectral imaging. As a specific use scenario, consider a tunable filter integrated remote temperature measurement system to collect calibrated multispectral images of air/spacecraft during ascent in order to validate the vehicle's thermal protection system. To make these measurements, state-of-

the-art systems rely on motorized filter wheels which rotate between several (typically ~ 5) single-notch optical filters. The filter wheels offer no real-time tunability and are limited in bandwidth, therefore missing out on important spectral and temporal data.

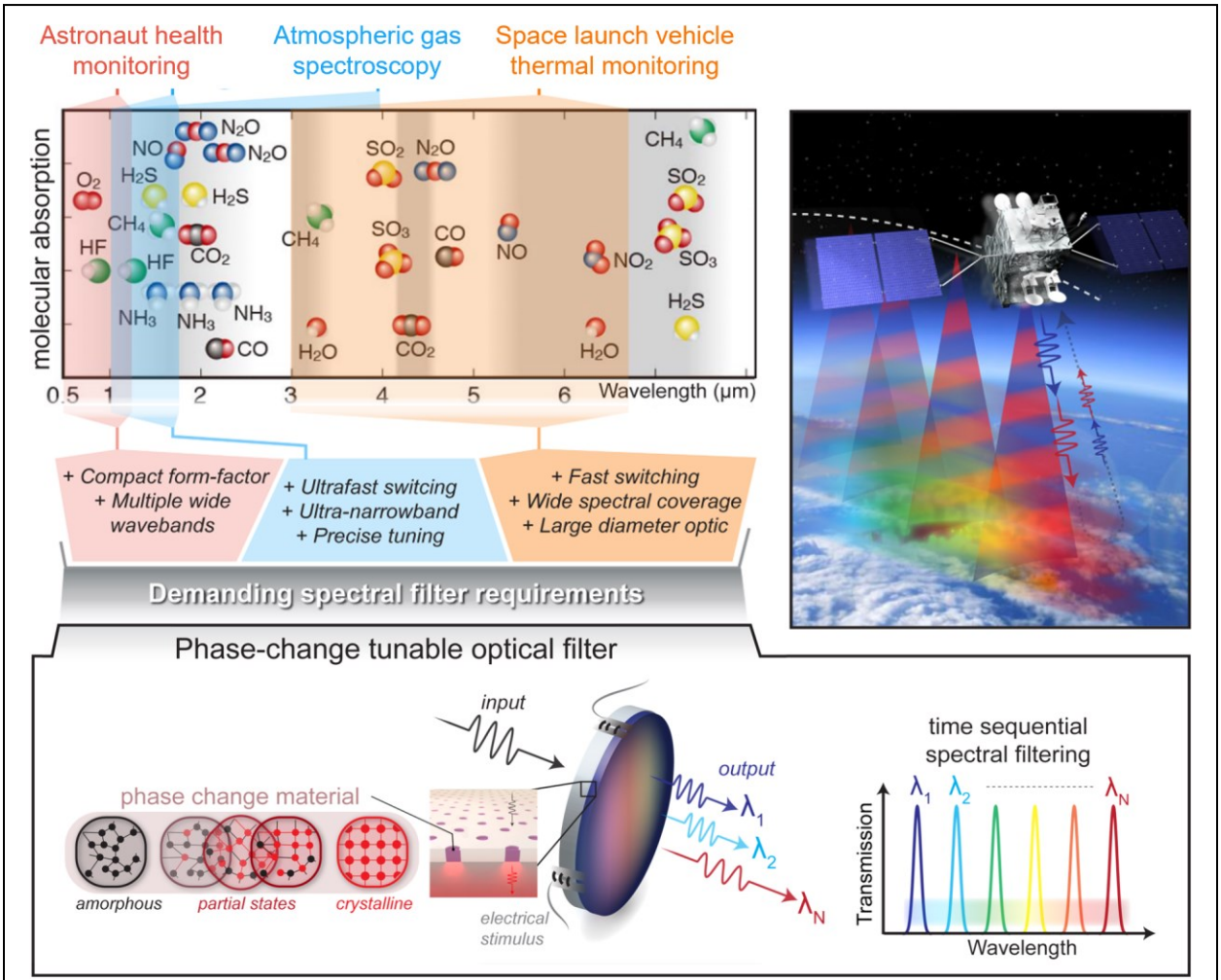

Fig. 2. Tunable metasurface filter for aerospace applications. Top-left: Characteristic absorption bands of molecules of interest to aerospace applications as well as application-specific requirements on the tunable spectral filter; top-right: satellite-based multispectral imaging for monitoring of atmospheric gas species; bottom: operating principle of the PCM-based metasurface filter: the PCM's structure can be continuously tuned in a non-volatile manner via voltage pulses, thereby spectrally shifting the passband of the metasurface. λ_1 to λ_N represent a series of transmission wavelengths that the filter scans through.

Recently, PCM-integrated tunable filters have shown promise as multifunctional wide-band replacements for bulky filter wheels in spaceborne remote sensing sub-systems[7,31,32] (Fig. 2). This is achieved through the integration of PCM into a plasmonic nanohole metasurface to tune the transmission passband in real time. Even though the existing PCM filter prototype is laser switched, its integration with on-chip micro-heaters will lead to orders-of-magnitude reduction in total SWaP[16]. The filters can be tuned within microseconds, enabling real-time thermography and imaging spectroscopy with high data throughput. Furthermore, LiDAR missions can utilize the same filters for chemical remote sensing, where the broadband tuning capability of the PCM-based filters provides unprecedented views of earth's atmospheric constituents and surface altimetry.

These features envisage that spaceborne systems incorporating PCM-based tunable filters will continue to be in demand into the foreseeable future with broad applications covering atmospheric gas sensing, space launch vehicle thermal imaging, and astronaut health monitoring.

- *Case Study 2: reconfigurable metasurfaces for beam steering*

Optical beam steering devices are gaining importance by the day with prospective applications in LiDAR for autonomous vehicles, remote sensing, and displays in AR/VR modules. A common embodiment of metasurface-based beam steering is to use the metasurface as an optical phased array (OPA). For a normal incident input beam with wavelength λ, the deflection angle θ is:

$$\frac{2\pi}{\lambda} \cdot \sin\theta = \frac{\Delta\varphi \pm m \cdot 2\pi}{\Lambda} \tag{1}$$

where Λ is the meta-atom pitch, $\Delta\varphi$ gives the phase delay between two neighbouring meta-atoms ($0 \leq \Delta\varphi < 2\pi$), and m denotes the aliasing order. Ideally, the equation should only be satisfied when $m = 0$, yielding a single solution of θ to eliminate aliasing. In an OPA with a FOV covering $-\theta_{max}$ to θ_{max}, the solution uniqueness condition becomes:

$$\Lambda = \frac{\lambda}{2\sin\theta_{max}} \tag{2}$$

A small pitch Λ is therefore instrumental to suppressing aliasing and increasing FOV, a unique advantage of metasurfaces over their classical diffractive counterpart. Another benefit of a small pitch is that the wavefront can be more precisely sculpted at a deep sub-wavelength scale, thereby enhancing efficiency[33]. This is particularly important for beam steering at large angles, where the wavefront follows a rapid spatial variation.

Besides efficiency, aliasing suppression and FOV, the main performance requirements for beam steering devices include beam divergence (which impacts angular resolution), speed, and reliability. Beam divergence is specified by the aperture size which scales with the number of meta-atoms and hence complexity of active control, while speed and reliability relate to the metasurface tuning mechanism. For automotive applications, an angular resolution of 0.2˚ or better is necessary, which translates to an aperture size of ~ 200 μm or larger for near-infrared LiDAR. Other specifications include a baseline frame rate of 10 Hz (or higher) and a typical combined (horizontal) FOV of 120˚. Compliance with reliability standards set forth by IEC (International Electrotechnical Commission), ISO (International Organization for Standardization), ASTM International and individual auto manufacturers further mandates tolerance against temperature excursions, mechanical shock, vibrations, fatigue, dust, and salt mist. The reduced temperature sensitivity (as compared to traditional refractive optics) and structural ruggedness of metasurfaces present an additional edge.

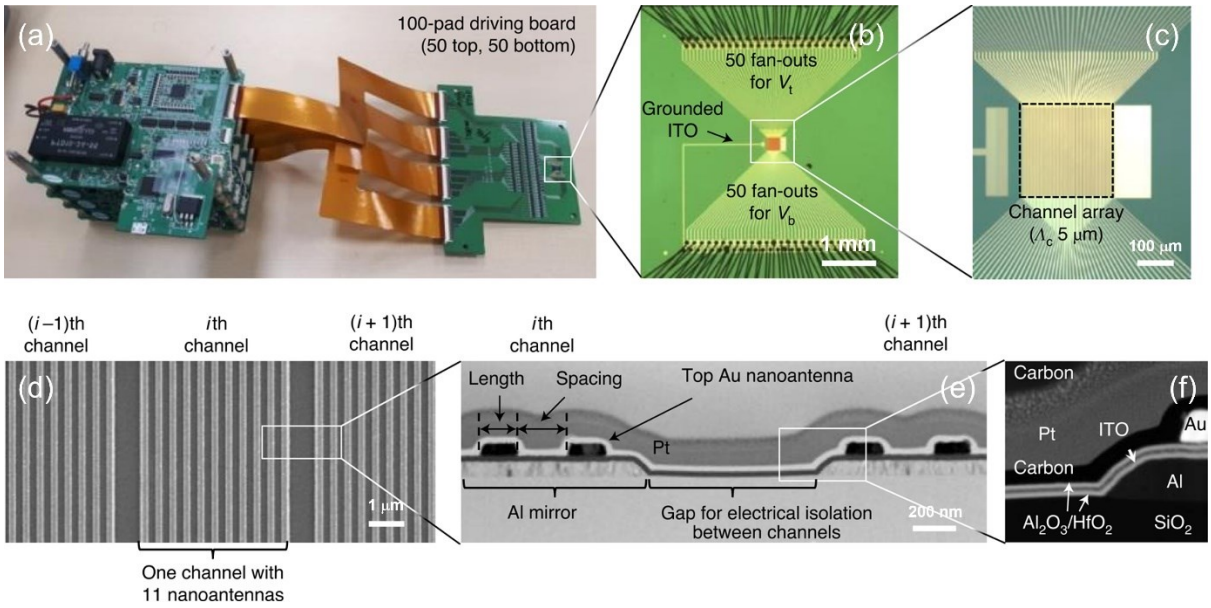

Fig. 3. Reconfigurable metasurfaces for beam steering. (a) Reconfigurable metasurface array mounted on an electronics board capable of independently driving 50 channels (pixels) with a pitch of Λ_c = 5 μm; (b, c) optical microscopy images of the array; (d) scanning electron microscopy image showing the 1-D pixels, each consisting of 11 meta-grating lines; (e, f) transmission electron microscopy images showing cross-sectional structures of the active array[5].

Several metasurface beam steering prototypes have been demonstrated. Li *et al.* developed a 1-D phase-only SLM based on a LC-infiltrated TiO_2 Huygens metasurface with an aperture size of 120 μm × 100 μm[34]. Each electrically addressed pixel comprise three rows of meta-atoms with a combined width of ~ 1 μm. The device achieves a diffraction efficiency of 36% at 660 nm wavelength and a FOV of 22˚. In parallel, Lumotive, a start-up focusing on LiDAR technologies, has been developing a "Meta-LiDAR" platform based on LCoS[35]. While details of the technology are not available in the public domain, their patents describe LC-infiltrated metal antenna arrays as the active beam steering element.

Beam steering at higher speed warrants alternative mechanisms. Researchers from Samsung demonstrated active 1-D meta-gratings made of indium tin oxide (ITO), where each individually contacted pixel contains 11 grating lines (Figs. 3a-f)[5]. A dual gate configuration was employed to realize independent control of phase and amplitude, a useful feature enabling apodization and sidelobe suppression. An RC-limited 3-dB bandwidth of 170 kHz was attained in a 200 μm × 200 μm device with a FOV of 15.4˚ and a diffraction efficiency of approximately 1%. 2-D beam steering based on a similar mechanism was also reported recently[36].

Before these pioneering demonstrations can enter the commercial realm, considerable performance improvements are anticipated. Down scaling the pixel size to the single meta-atom level will fully leverage the promised advantages of metasurface OPAs such as aliasing-free operation, high efficiency and large FOV. Angle-dependent and nonlocal metasurface designs will further enhance the performance of large-angle steering systems. A scalable electrical addressing scheme commensurate with large aperture active tuning is sought after to enhance resolution and facilitate agile 2-D beam steering. Finally, reliable packaging suitable for field deployment must be validated.

- *Case Study 3: reconfigurable metasurface enabled glasses-free 3-D display*

Glasses-free 3-D display (autostereoscopy) is a technology poised to reshape human-machine interactions. Unlike conventional display panels which reproduce only the intensity of light emanating from an object, an autostereoscopic display restores the light field information including both intensity and propagation direction. The schematic configuration of a 3-D display is depicted in Fig. 4a. A pixel modulates the light output intensity and at the same time directs emitted light to a specific direction. Therefore, the pixels can be grouped according to their emission directions. Each subset of pixels projects a unique perspective view of the displayed scene along one viewing angle (and hence the name "multiview display"), thereby creating 3-D stereoscopic perception for users. Early prototypes of multiview display were implemented using parallax barriers, lenticular lenses or micro-lens arrays on top of flat display panels, although they face limitations in efficiency, FOV and depth of field. Moreover, spatial and angular resolutions represent an inherent trade-off, since the spatial resolution is reduced by a factor equalling to the number of angular views. The subpar spatial and angular resolution is a primary factor that degrades user experience.

The challenges encountered by traditional optics have fuelled a growing interest in multiview displays based on flat optics. A group from HP Laboratories first reported 3-D display using arrays of diffractive grating pixels in place of refractive optics[37], providing 64-view images within 90˚ FOV. Notwithstanding the passive nature of the grating pixels, they were integrated with an active LC shutter plane to perform dynamic image display. This innovation has been successfully commercialized by Leia Inc.[38]. Using metasurfaces as the light-directing agent promises several additional benefits. While the efficiency of traditional diffraction gratings is limited by power dissipation into high-order diffraction, metasurfaces avoid undesirable diffraction orders to significantly boost efficiency and reduce background noise. The exceptional light bending capability of metasurfaces affords a large FOV without compromising efficiency. For example, recent work by Hua *et al.* demonstrated a metasurface-enabled full-colour 3-D display prototype with a record 160˚ horizontal FOV (Figs. 4b and 4c)[39]. Metasurfaces also allow densely packed pixels with a large fill factor to improve display resolution without inducing excessive crosstalk, and they can further exploit temporal and polarization multiplexing schemes to alleviate the trade-off between spatial and angular resolution[40]. Additionally, metasurface pixel arrays with tunable light directing properties can be coupled with an eye tracking sensor such that the number of angular views broadcasted toward the observer is dynamically optimized. Yet another potential advantage of metasurfaces is the prospect of their monolithic integration on display pixels such as micro-LEDs[41,42], which opens up unprecedented latitude for fine control of the emission light field.

In sum, high-density, efficient metasurface optics offer a promising route to solve the resolution bottleneck of 3-D displays and catalyse their widespread adoption in next-generation consumer electronic devices. 3-D display also presents an enticing opportunity (and challenge) for metasurface-augmented, large-scale 2-D pixel arrays, as we elaborate in the following sections.

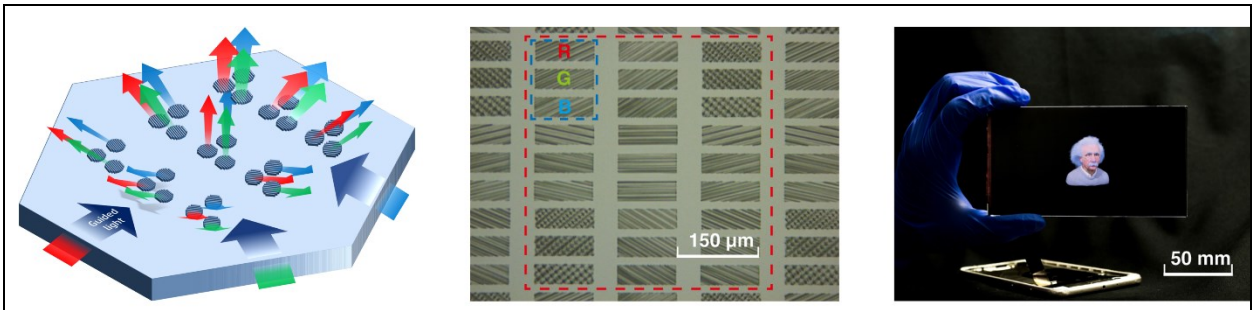

Fig. 4. Metasurface-based 3-D display. (a) Schematic design of a multi-view 3-D display panel consisting of metasurface pixel arrays[37]; (b) optical microscopy image of tri-color metasurface pixel arrays[39]; (c) a full-colour, video-rate 3-D display prototype[39].

Outstanding technological challenges

Despite the explosive growth of reconfigurable metasurface technologies over the past few years, several technological gaps still loom. Here we focus on three critical areas where more R&D efforts are mandated before the application prospects portrayed in the last section can be fulfilled.

- *Scalable manufacturing and packaging*

The first and foremost barrier lies in scalable manufacturing and packaging of reconfigurable metasurfaces. Their passive counterparts used to encounter the same challenge: in the early phase of development, metasurfaces were almost exclusively prototyped in university cleanrooms using electron beam lithography with painstakingly low throughput. Recent advances have nonetheless circumvented this bottleneck, as fabrication of passive metasurfaces on full glass wafers have been validated via deep ultraviolet lithography in silicon foundries[43,44] and other high-throughput fabrication methods such as nanoimprint lithography[45] have been implemented as well. Manufacturing of reconfigurable metasurfaces not only stipulates similar requirements on large-area, fine-line lithographic patterning, but is also appreciably more complicated than their passive counterpart. Therefore, commercially viable manufacturing practices of reconfigurable metasurfaces will need to maximally leverage standard semiconductor processing and packaging to manage the escalating fabrication and assembly complexity. The foundry manufacturing process may be complemented with backend integration to introduce new materials and functions, in which case the integration process shall capitalize on a mature industrial ecosystem (summarized in Table 1) to access existing infrastructures, knowledge base, and supply chain to expedite the technology's learning curve.

- *Electrical addressing of large 2-D pixel arrays*

Scaling the existing reconfigurable metasurface technologies to electrically controlled, high-density and large-size 2-D pixel arrays marks another technical milestone. This is motivated by the demand for enhanced wavefront control with fine resolution: taking beam steering as an example, reducing pixel size contributes to expanding FOV and suppressing sidelobes. At the limit when each meta-atom can be individually tuned (i.e. one meta-atom per pixel), a 'universal' optic results, enabling not only continuous tuning but also reconfiguration of the metasurface to emulate arbitrary optics.

The Holy Grail of a 'universal optic', however, faces major challenges in electrical wiring, cross-talk, and control complexity. In-plane fan-out wiring designs have been adopted to demonstrate 1-D reconfigurable metasurfaces[5,9,11,34,46] and recently a small (10 × 10 pixels) 2-D

array[36], although the layout is not scalable to large 2-D matrices. A practical solution for large 2-D arrays involves integrating the pixels to a control backplane via vertical interconnect accesses to form a cross-bar matrix. In the case of volatile pixels, each pixel needs to be coupled with a transistor such that its can be individually tuned, analogous to the active matrix architecture in flat panel displays. For nonvolatile reconfigurable metasurfaces, a simplified 'passive matrix' configuration without the transistor backplane is equally viable since the 'set-and-forget' pixels can be reconfigured sequentially row-by-row, albeit at the expense of refreshing rate. Notably, each pixel in a passive-matrix cross-bar array still requires a selector with unipolar or nonlinear I-V characteristics to prevent sneak-path current, which can be implemented via diodes or threshold switching phenomena in various materials.

It is worth mentioning that continuous tuning of a meta-optical element does not necessarily entail full 2-D matrix addressing. For instance, modulating the phase delay gradient between electrode pairs rather than the phase delay at individual meta-atom pixels can dramatically reduce the number of electrical leads and hence wiring complexity. Using this scheme, a metalens with 1 mm diameter and 24 electrical contacts was designed[47]. It is capable of continuous focal length tuning from 2 mm to infinity at 2.2 μm wavelength while maintaining diffraction-limited performance throughout. In contrast, 2-D addressing of a metalens of the same size involve a staggering half million active pixels!

- *Reliability and endurance*

Last but certainly not least comes reliability, a topic rarely deliberated in academic publications. Nevertheless, its importance to practical applications cannot be over-emphasized. The reliability requirement is illustrated in the example of automotive LiDAR, whose durability qualifications under various environmental stresses are elaborately enumerated by international standards and manufacturers' specifications. For reconfigurable metasurfaces, endurance is another critical parameter. As is evident from Tables 1 and 2, the endurances of many reconfigurable metasurface technologies are still lagging application demands. Even for those labelled with 'very large' endurance, their reliability under realistic deployment conditions has often not been verified.

Addressing the reliability challenge warrants scrupulous characterization of degradation kinetics in application-relevant environments, thorough material investigations to elucidate the pertinent failure mechanisms, and judicious device designs guided by the fundamental insights to improve robustness. The studies will inform the essential path for reconfigurable metasurfaces to make a lasting impact on photonic applications.

New capabilities beyond today's functional repertoire

In addition to filling the missing links, new research initiatives in the field are set to significantly expand the functionalities of reconfigurable metasurface optics. In this section, we highlight two salient examples where such advances are anticipated to enhance their performances and open up novel application venues.

- *Dual modulation of phase and amplitude*

Even though imparting a phase delay without incurring optical loss is a common design prescription for phase-gradient metasurfaces, there are scenarios where simultaneous phase and amplitude modulation comes in handy. In OPAs, amplitude apodization helps to match the output field profile to that of a Gaussian beam to suppress sidelobes. In 3-D display, the dual modulation is the prerequisite for complete light field manipulation. In analog optical computing, both phase and amplitude are often concurrently used to encode information[1].

One solution involves using two cascaded reconfigurable metasurfaces. For example, it has been shown that independent amplitude and phase modulation of an incident plane wave can be attained with two phase-only metasurfaces with minimal optical loss[48]. Alternatively, a dual-gate configuration has been applied to ITO metasurfaces to accommodate complex reflectance tuning by adjusting two gate voltages[5,49], although the coupled refractive index and absorption changes due to free carrier dispersion in ITO restricts the accessible tuning range. Resorting to two distinct mechanisms to separately engineer refractive index and loss furnishes far more versatile phase and amplitude control. Candidate materials include ionic conductors where migration of different ions produces tri-state switching with orthogonal optical property changes[50], and chalcogenide PCMs where crystallization and vacancy ordering account for decoupled refractive index and absorption modifications[51].

- *Metasurface-augmented active photonics*

While useful as standalone optical elements, the application scope of reconfigurable metasurfaces can be significantly broadened once they can be seamlessly integrated with traditional optical or optoelectronic components. Such metasurface-augmented photonics transcends intrinsic performance limits confronting metasurfaces, such as narrow spectral bandwidth and low quality factor (Q): combining metasurfaces with refractive or reflective optics overcomes their group delay limitation[52] to support broadband operation[53], and embedding active meta-atoms inside a Fabry-Perot cavity maintains the otherwise wavelength-sensitive high-Q resonance condition across a wide tuning range[54]. Besides the performance gains, metasurfaces further profit from their compatibility with monolithic or hybrid integration on optoelectronic platforms including lasers[55], planar photonic integrated circuits[56], as well as display and imaging arrays[42,57]. The integration can potentially leverage scalable semiconductor fabrication routes to access sophisticated electronic backplanes for massive array modulation. Moreover, some tuning operations (in particular amplitude modulation) can be offloaded to the optoelectronic components to simplify the meta-optical system while retaining active functionalities (e.g., in a metasurface-integrated micro-LED multi-view display). We envision that the metasurface-augmented optoelectronic systems will confer novel capabilities such as pixel-level light field control and detection, computational imaging, high-resolution imaging spectroscopy, and neuromorphic computing.

Realizing the metasurface-augmented active photonics calls for innovative design and fabrication strategies. Specifically, two modelling frameworks are essential to metasurface-augmented photonics. One is a computationally efficient objective-driven method to approach this inherently multiscale – spanning six orders of magnitude in spatial dimensions – and multi-objective – as specified by the active tuning condition – design problem. A successful recipe will likely bridge classical ray based optimization of traditional optics and emerging full-wave inverse design techniques for sub-wavelength meta-structures[58–60]. The other involves multi-physics *predictive* models linking the (electrical, thermal, mechanical, and/or optical) stimuli to the resulting metasurface response, which becomes particularly important in treating complex material transformations where simple effective medium theory fails[61,62].

Advancing metasurface-augmented photonics also demands fabrication schemes commensurate with scalable manufacturing, such as conformal processing of metasurfaces on both flat and curved surfaces of conventional optics, and monolithic integration routes of meta-optics on optoelectronic devices[57]. We foresee that breakthroughs in scalable metasurface integration will catalyse new applications exploiting the best of two worlds in both conventional optics and metasurfaces.

Summary and outlook

Since their introduction in the past decade, reconfigurable metasurfaces have swiftly taken the centre stage in metamaterials research, boasting significantly enhanced and expanded functionalities over their passive counterparts. The extra layer of complexity needed for active tuning, however, presents an additional barrier to their deployment in the commercial domain.

To overcome the challenges, the imminent success of passive metasurfaces, whose industrial applications start to surface, sets a paradigm. Over the past few years, the community has converged upon several potential beachhead markets of passive metasurfaces where their key competitive advantages – system-level SWaP benefits, minimal monochromatic aberration, polarization discrimination capacity, and low-cost at scale – are fully mobilized, and forged a path toward large-area, cost-effective manufacturing capitalizing on standard foundry processing. Likewise, leveraging existing semiconductor foundry infrastructures as well as mature ecosystems in adjacent industries provide a shortcut to facilitate scalable manufacturing and packaging of reconfigurable metasurface devices. As reconfigurable metasurfaces establish their manufacturing scalability and reliability, their industrial deployment will also be initiated in niche applications, with several promising early examples discussed in the text, before percolating into established markets. In this process, new and unique functionalities exemplified by ‘universal optics’ consisting of 2-D active meta-atom pixel arrays, electronics and optoelectronics with monolithically integrated metasurface optics, and flat optics rendering complete active control of light phase and amplitude will continue to extend their applications. The growing market demands will in turn drive the assimilation of reconfigurable metasurface fabrication into mainstream foundry processes to further enhance yield, lower cost, and improve reliability toward widespread adoption of the technology. This is a bright prospect that the entire active metasurface community can and should strive for, as ‘the future depends on what we do in the present’.

Table 1. Summary of reconfigurable metasurface technologies: the endurance and bandwidth values are quoted for optical devices with best-in-class performance on the specific metric and do not necessarily represent fundamental limits of the technologies[a]

Type	Material or mechanism	Refractive index tuning range	Optical absorption	Endurance (cycling lifetime)	3-dB bandwidth or 10-90 rise/fall time[b]	Potential challenges	Relevant industry ecosystem
Mechanical	Displacement	-	None[c]	Very large	~ 1 Hz	Integration challenge	-
	Elastic deformation	-	None[c]	15,000[63]	~ 1 Hz	Reproducibility and stability	-
	MEMS actuation	-	None[c]	> 10^9 [64]	1 MHz[64]	High voltage	MEMS
Free carrier density modulation (electrical injection)	Semiconductors (junction biasing)	~ 0.1	Free carrier absorption (FCA)	Very large	0.18 MHz[65]	Optical loss; small index change or optical modal overlap with the active region	Semiconductor
	TCOs (field gating)	1.39[66]	FCA	Very large	10 MHz[67]		Display
	2-D materials (field gating)	~ 1 at room temperature[68,69] Up to ~ 5 at low temperature[70]	Material absorption and FCA	Very large	> 1 GHz[71]		-
Thermo-optic	Semiconductors (thermal free-carrier refraction)	1.5[72]	FCA	Likely large	5 kHz[73]	Optical loss; relatively slow response	Integrated photonics
	Semiconductors or dielectric materials	0.15[74]	Minor FCA due to carrier thermalization			Relatively slow response; large energy consumption	
Electro-optic	EO polymers	~ 0.1[75]	None[c]	Very large	50 MHz[75,76]	High voltage	-
	EO crystals	0.001[77]	None[c]	Very large	95 MHz[78]	Small modulation amplitude	Integrated photonics
	Liquid crystals	0.15[79,80]	None[c]	> 10^{10}	350 Hz[81]	Relatively slow response	Display
	Semiconductor multi-quantum-well (quantum confined Stark effect)	~ 0.01[11]	Electroabsorption dictated by the Kramers-Kronig relations	Very large	< 10 ns[82]	Full 2π phase coverage	III-V optoelectronics
Phase transition	VO_2	Up to ~ 0.5 in visible and near-infrared[83]	FCA in the metallic state	> 24,000[84]	450 fs / 2 ps[85]	Optical loss	-
	Chalcogenide PCMs	3.3 ($Ge_2Sb_2Te_5$)[86] 1.8 ($Ge_2Sb_2Se_4Te$)[87]	None[c]	> 5×10^5 [88]	200 ns / 300 ns[89]	High voltage	Memory
Electrochemical	Electrochromic polymers	0.7[90]	Electronic absorption at the oxidized state	> 10^7 [91]	> 25 Hz[91]	Relatively slow response; optical loss	Smart windows
	Ionic conducting oxides (protonation)	0.45 ($SmNiO_3$)[92] ~ 0.4 (GdO_x)[93]	FCA in the metallic state	Several hundred[93]	13 ms[93]	Endurance; relatively slow response	-
	Ionic conducting oxides (lithium intercalation)	~ 0.2 (WO_3)[94] 0.65 (TiO_2)[95]	FCA in the metallic state	400[95]	3 s[96]	Endurance; slow response	Smart windows
	Metal electrodeposition	-	Absorption of electrodeposited metal	> 200[97]	~ 1 Hz[97]	Integration challenge	-
Chemical	Metals (hydrogenation)	~ 4 (Mg)[98]	FCA	3,000[99]	~ 0.1 Hz[100]	Integration challenge	-
	Cover material addition/removal	~ 0.5[101,102]	None[c]	> 10 [103]	Seconds to minutes	Integration challenge	-
Magnetic	Magnetooptical oxides	~ 0.01[104]	None[c]	Very large	5 GHz[105]	Integration challenge	-
All-optical	Kerr nonlinearity	Light intensity dependent	Nonlinear absorption	Very large	40 fs[106]	Integration challenge	-
	Free carrier injection	0.14[107]	FCA	Very large	~ 100 fs / 20 ps[108]	Integration challenge	-

[a] Here we focus on reconfigurable metasurfaces operating in the optical frequency range, specifically from ultraviolet to long-wave infrared (excluding the terahertz spectrum). Only experimental demonstrations are included in the table. Refer to Ref. [47] for more information and discussions.

[b] In the case of reconfigurable metasurfaces with asymmetric rise/fall responses, both rise and fall time values are reported.

[c] Here 'none' implies that the optical loss *can be* negligible throughout the entire active tuning cycle. However, this condition does not necessarily hold for all materials or devices belonging to the category.

Table 2. Potential applications of reconfigurable metasurfaces: green-yellow-grey colours indicate decreasing relevance of the metric to the target use case: very important-somewhat important-minimally relevant[a]

Application	Tuning scheme	Optical tuning parameter (phase/amplitude)	Optical contrast (relevant metrics)	Optical loss suppression	Endurance (cycling lifetime requirement)	Speed (bandwidth requirement)	Power consumption
Tunable filters for multispectral sensing	Continuous	Amplitude	Extinction ratio		10^7	1 kHz	
Beam steering for LiDAR	Continuous	Both	Full 2π phase tuning range		10^9	10 Hz	
Light field display	Continuous	Both	Field-of-view and image contrast		10^{10}	30 Hz	
Computational imaging	Discrete	Phase	Full 2π phase tuning range		10^{10}	100 Hz	
Optical neural network with adaptive network training	Continuous	Both	Full 2π phase tuning range		10^8	1 kHz	
Dynamic projection display	Continuous	Amplitude	Image contrast		10^{10}	30 Hz	
Electronic paper (reflective display)	Discrete or continuous	Amplitude	Color saturation and image contrast		10^7	1 Hz	Nonvolatile or capacitive
Zoom lens	Discrete or continuous	Phase	Full 2π phase tuning range		10^5	1 Hz	
Digital signal modulation for free-space communications	Discrete	Either	Modulation contrast		10^{18}	10 GHz	
Adaptive optics	Continuous	Phase	Full 2π phase tuning range		10^{10}	100 Hz	
Nonreciprocal optics based on spatiotemporal modulation	Discrete	Either	Isolation ratio		10^{18}	10 GHz	
Optical limiter	Discrete	Amplitude	Extinction ratio		Application-specific	> 1 GHz	Nonvolatile
Adaptive thermal camouflage	Continuous	Amplitude	Dynamic range		10^8	10 Hz	

[a] Refer to Ref. [47] for more information and discussions.

References

1. Abdollahramezani, S., Hemmatyar, O. & Adibi, A. Meta-optics for spatial optical analog computing. *Nanophotonics* **9**, 4075–4095 (2020).
2. Salary, M. M. & Mosallaei, H. Time-Modulated Conducting Oxide Metasurfaces for Adaptive Multiple Access Optical Communication. *IEEE Trans. Antennas Propag.* **68**, 1628–1642 (2020).
3. Liu, Y. *et al.* Dynamic thermal camouflage via a liquid-crystal-based radiative metasurface. *Nanophotonics* **9**, 855–863 (2020).
4. Shalaginov, M. Y. *et al.* Reconfigurable all-dielectric metalens with diffraction-limited performance. *Nat. Commun.* **12**, 1225 (2021).
5. Park, J. *et al.* All-solid-state spatial light modulator with independent phase and amplitude control for three-dimensional LiDAR applications. *Nat. Nanotechnol.* **16**, 69–76 (2020).
6. Gyeongtae Kim *et al.* Metasurface-empowered spectral and spatial light modulation for disruptive holographic displays. *Nanoscale* **14**, 4380–4410 (2022).
7. Julian, M. N., Williams, C., Borg, S., Bartram, S. & Kim, H. J. Reversible optical tuning of GeSbTe phase-change metasurface spectral filters for mid-wave infrared imaging. *Optica* **7**, 746–754 (2020).
8. Wang, X., Díaz-Rubio, A., Li, H., Tretyakov, S. A. & Alù, A. Theory and Design of Multifunctional Space-Time Metasurfaces. *Phys. Rev. Appl.* **13**, 044040 (2020).
9. Shirmanesh, G. K., Sokhoyan, R., Wu, P. C. & Atwater, H. A. Electro-optically Tunable Multifunctional Metasurfaces. *ACS Nano* **14**, 6912–6920 (2020).
10. Weiss, A. *et al.* Tunable Metasurface Using Thin-Film Lithium Niobate in the Telecom Regime. *ACS Photonics* **9**, 605–612 (2022).
11. Wu, P. C. *et al.* Dynamic beam steering with all-dielectric electro-optic III–V multiple-quantum-well metasurfaces. *Nat. Commun.* **10**, 3654 (2019).
12. Bosch, M., Shcherbakov, M. R., Fan, Z. & Shvets, G. Polarization states synthesizer based on a thermo-optic dielectric metasurface. *J. Appl. Phys.* **126**, 073102 (2019).
13. Kaissner, R. *et al.* Electrochemically controlled metasurfaces with high-contrast switching at visible frequencies. *Sci. Adv.* **7**, eabd9450 (2021).
14. Xia, S. *et al.* Enhancement of the Faraday Effect and Magneto-optical Figure of Merit in All-Dielectric Metasurfaces. *ACS Photonics* **9**, 1240–1247 (2022).
15. Tripathi, A. *et al.* Tunable Mie-Resonant Dielectric Metasurfaces Based on VO2 Phase-Transition Materials. *ACS Photonics* **8**, 1206–1213 (2021).
16. Zhang, Y. *et al.* Electrically reconfigurable non-volatile metasurface using low-loss optical phase-change material. *Nat. Nanotechnol.* **16**, 661–666 (2021).
17. Komar, A. *et al.* Dynamic Beam Switching by Liquid Crystal Tunable Dielectric Metasurfaces. *ACS Photonics* **5**, 1742–1748 (2018).
18. Waters, R. F., Hobson, P. A., MacDonald, K. F. & Zheludev, N. I. Optically switchable photonic metasurfaces. *Appl. Phys. Lett.* **107**, 081102 (2015).
19. Colburn, S., Zhan, A. & Majumdar, A. Varifocal zoom imaging with large area focal length adjustable metalenses. *Optica* **5**, 825–831 (2018).
20. Malek, S. C., Ee, H.-S. & Agarwal, R. Strain Multiplexed Metasurface Holograms on a Stretchable Substrate. *Nano Lett.* **17**, 3641–3645 (2017).
21. Arbabi, E. *et al.* MEMS-tunable dielectric metasurface lens. *Nat. Commun.* **9**, 812 (2018).
22. He, Q., Sun, S. & Zhou, L. Tunable/Reconfigurable Metasurfaces: Physics and Applications. *Research* **2019**, 1–16 (2019).

23. Zahra, S. *et al.* Electromagnetic Metasurfaces and Reconfigurable Metasurfaces: A Review. *Front. Phys.* **8**, 615 (2021).
24. Hu, J., Bandyopadhyay, S., Liu, Y. H. & Shao, L. Y. A Review on Metasurface: From Principle to Smart Metadevices. *Front. Phys.* **8**, 502 (2021).
25. Paniagua-Domínguez, R. *et al.* A Metalens with a Near-Unity Numerical Aperture. *Nano Lett.* **18**, 2124–2132 (2018).
26. Liang, H. *et al.* Ultrahigh Numerical Aperture Metalens at Visible Wavelengths. *Nano Lett.* **18**, 4460–4466 (2018).
27. Shalaginov, M. Y. *et al.* Single-Element Diffraction-Limited Fisheye Metalens. *Nano Lett.* **20**, 7429–7437 (2020).
28. Lin, Z. *et al.* End-to-end nanophotonic inverse design for imaging and polarimetry. *Nanophotonics* **10**, 1177–1187 (2021).
29. Arya, G. *et al.* End-to-End Optimization of Metasurfaces for Imaging with Compressed Sensing. *arXiv:2201.12348* (2022).
30. Shalaginov, M. Y. *et al.* Design for quality: reconfigurable flat optics based on active metasurfaces. *Nanophotonics* **9**, 3505–3534 (2020).
31. Williams, C., Hong, N., Julian, M., Borg, S. & Kim, H. J. Tunable mid-wave infrared Fabry-Perot bandpass filters using phase-change GeSbTe. *Opt. Express* **28**, 10583 (2020).
32. Rais-Zadeh, M. & Jafari, M. Zero-static-power phase-change optical modulator. *Opt. Lett.* **41**, 1177–1180 (2016).
33. Chung, H. & Miller, O. D. High-NA achromatic metalenses by inverse design. *Opt. Express* **28**, 6945–6965 (2020).
34. Li, S. Q. *et al.* Phase-only transmissive spatial light modulator based on tunable dielectric metasurface. *Science* **364**, 1087–1090 (2019).
35. Lumotive. Available at: https://www.lumotive.com/.
36. Kim, S. Il *et al.* Two-dimensional beam steering with tunable metasurface in infrared regime. *Nanophotonics* **11**, 2719–2726 (2022).
37. Fattal, D. *et al.* A multi-directional backlight for a wide-angle, glasses-free three-dimensional display. *Nature* **495**, 348–351 (2013).
38. Lume Pad 3D Lightfield Tablet | Leia Inc. Available at: https://www.leiainc.com/.
39. Hua, J. *et al.* Foveated glasses-free 3D display with ultrawide field of view via a large-scale 2D-metagrating complex. *Light Sci. Appl.* **10**, 213 (2021).
40. Hua, J., Qiao, W. & Chen, L. Recent Advances in Planar Optics-Based Glasses-Free 3D Displays. *Front. Nanotechnol.* **4**, 829011 (2022).
41. Khaidarov, E. *et al.* Control of LED Emission with Functional Dielectric Metasurfaces. *Laser Photon. Rev.* **14**, 1900235 (2020).
42. Joo, W. J. *et al.* Metasurface-driven OLED displays beyond 10,000 pixels per inch. *Science* **370**, 2022 (2020).
43. Park, J. S. *et al.* All-Glass, Large Metalens at Visible Wavelength Using Deep-Ultraviolet Projection Lithography. *Nano Lett.* **19**, 8673–8682 (2019).
44. Hu, T. *et al.* CMOS-compatible a-Si metalenses on a 12-inch glass wafer for fingerprint imaging. *Nanophotonics* **9**, 823–830 (2020).
45. Verschuuren, M. A., Knight, M. W., Megens, M. & Polman, A. Nanoscale spatial limitations of large-area substrate conformal imprint lithography. *Nanotechnology* **30**, 345301 (2019).
46. Thureja, P. *et al.* Array-level inverse design of beam steering active metasurfaces. *ACS*

Nano **14**, 15042–15055 (2020).
47. Gu, T., Kim, H. J., Rivero-Baleine, C. & Hu, J. Active metasurfaces: lighting the path to commercial success. *arXiv:2205.14193* (2022).
48. Raeker, B. O. *et al.* All-Dielectric Meta-Optics for High-Efficiency Independent Amplitude and Phase Manipulation. *Adv. Photonics Res.* **3**, 2100285 (2022).
49. Kafaie Shirmanesh, G., Sokhoyan, R., Pala, R. A. & Atwater, H. A. Dual-Gated Active Metasurface at 1550 nm with Wide (>300°) Phase Tunability. *Nano Lett.* **18**, 2957–2963 (2018).
50. Lu, N. *et al.* Electric-field control of tri-state phase transformation with a selective dual-ion switch. *Nature* **546**, 124–128 (2017).
51. Zhang, Y. *et al.* Myths and truths about optical phase change materials: A perspective. *Appl. Phys. Lett.* **118**, 210501 (2021).
52. Presutti, F. & Monticone, F. Focusing on Bandwidth: Achromatic Metalens Limits. *Optica* **7**, 624–631 (2020).
53. Chen, W. T. *et al.* Broadband Achromatic Metasurface-Refractive Optics. *Nano Lett.* **18**, 7801–7808 (2018).
54. An, S. *et al.* Deep neural network enabled active metasurface embedded design. *Nanophotonics* (2022). doi:10.1515/NANOPH-2022-0152
55. Wen, D. & Crozier, K. B. Metasurfaces 2.0: Laser-integrated and with vector field control. *APL Photonics* **6**, 080902 (2021).
56. Wu, C. *et al.* Programmable phase-change metasurfaces on waveguides for multimode photonic convolutional neural network. *Nat. Commun.* **12**, 96 (2021).
57. Kobayashi, F., Shikama, K., Miyata, M., Nemoto, N. & Hashimoto, T. Full-color-sorting metalenses for high-sensitivity image sensors. *Optica* **8**, 1596–1604 (2021).
58. Wu, K., Coquet, P., Wang, Q. J. & Genevet, P. Modelling of free-form conformal metasurfaces. *Nat. Commun.* **9**, 3494 (2018).
59. Campbell, S. D. *et al.* Review of numerical optimization techniques for meta-device design [Invited]. *Opt. Mater. Express* **9**, (2019).
60. Li, Z. *et al.* Inverse design enables large-scale high-performance meta-optics reshaping virtual reality. *Nat. Commun.* **13**, 2409 (2022).
61. Frame, J. D., Green, N. G. & Fang, X. Modified Maxwell Garnett model for hysteresis in phase change materials. *Opt. Mater. Express* **8**, 1988 (2018).
62. Meyer, S., Tan, Z. Y. & Chigrin, D. N. Multiphysics simulations of adaptive metasurfaces at the meta-atom length scale. *Nanophotonics* **9**, 675–681 (2020).
63. Martin-Monier, L., Gupta, T. Das, Yan, W., Lacour, S. & Sorin, F. Nanoscale Controlled Oxidation of Liquid Metals for Stretchable Electronics and Photonics. *Adv. Funct. Mater.* **31**, 2006711 (2021).
64. Holsteen, A. L., Cihan, A. F. & Brongersma, M. L. Temporal color mixing and dynamic beam shaping with silicon metasurfaces. *Science* **365**, 257–260 (2019).
65. Iyer, P. P., Pendharkar, M., Palmstrøm, C. J. & Schuller, J. A. III–V Heterojunction Platform for Electrically Reconfigurable Dielectric Metasurfaces. *ACS Photonics* **6**, 1345–1350 (2019).
66. Feigenbaum, E., Diest, K. & Atwater, H. A. Unity-Order Index Change in Transparent Conducting Oxides at Visible Frequencies. *Nano Lett.* **10**, 2111–2116 (2010).
67. Huang, Y.-W. *et al.* Gate-Tunable Conducting Oxide Metasurfaces. *Nano Lett.* **16**, 5319–5325 (2016).

68. Emani, N. K. *et al.* Electrically Tunable Damping of Plasmonic Resonances with Graphene. *Nano Lett.* **12**, 5202–5206 (2012).
69. Yu, Y. *et al.* Giant Gating Tunability of Optical Refractive Index in Transition Metal Dichalcogenide Monolayers. *Nano Lett.* **17**, 3613–3618 (2017).
70. Li, M., Biswas, S., Hail, C. U. & Atwater, H. A. Refractive Index Modulation in Monolayer Molybdenum Diselenide. *Nano Lett.* **21**, 7602–7608 (2021).
71. Zeng, B. *et al.* Hybrid graphene metasurfaces for high-speed mid-infrared light modulation and single-pixel imaging. *Light Sci. Appl.* **7**, 51 (2018).
72. Iyer, P. P., Pendharkar, M., Palmstrøm, C. J. & Schuller, J. A. Ultrawide thermal free-carrier tuning of dielectric antennas coupled to epsilon-near-zero substrates. *Nat. Commun.* **8**, 472 (2017).
73. Horie, Y., Arbabi, A., Arbabi, E., Kamali, S. M. & Faraon, A. High-Speed, Phase-Dominant Spatial Light Modulation with Silicon-Based Active Resonant Antennas. *ACS Photonics* **5**, 1711–1717 (2018).
74. Lewi, T., Butakov, N. A. & Schuller, J. A. Thermal tuning capabilities of semiconductor metasurface resonators. *Nanophotonics* **8**, 331–338 (2018).
75. Benea-Chelmus, I. C. *et al.* Electro-optic spatial light modulator from an engineered organic layer. *Nat. Commun.* **12**, 5928 (2021).
76. Tanemura, T., Zhang, J., Kosugi, Y., Ogasawara, M. & Nakano, Y. Metasurface high-speed modulators using electro-optic polymer. in *SPIE Proceedings* **11692**, 1169208 (SPIE, 2021).
77. Karvounis, A. *et al.* Electro-Optic Metasurfaces Based on Barium Titanate Nanoparticle Films. *Adv. Opt. Mater.* **8**, 2000623 (2020).
78. Karvounis, A., Vogler-Neuling, V. V. & Grange, R. 95 MHz Bandwidth Electro-Optic Metasurfaces based on Barium Titanate Nanocrystals. in *2021 Conference on Lasers and Electro-Optics, CLEO 2021 - Proceedings* FTh4K.5 (Optica Publishing Group, 2021). doi:10.1364/cleo_qels.2021.fth4k.5
79. Li, J., Wu, S. T., Brugioni, S., Meucci, R. & Faetti, S. Infrared refractive indices of liquid crystals. *J. Appl. Phys.* **97**, 073501 (2005).
80. Buchnev, O., Podoliak, N., Kaczmarek, M., Zheludev, N. I. & Fedotov, V. A. Electrically Controlled Nanostructured Metasurface Loaded with Liquid Crystal: Toward Multifunctional Photonic Switch. *Adv. Opt. Mater.* **3**, 674–679 (2015).
81. Kowerdziej, R., Wróbel, J. & Kula, P. Ultrafast electrical switching of nanostructured metadevice with dual-frequency liquid crystal. *Sci. Rep.* **9**, 20367 (2019).
82. Lee, J. *et al.* Ultrafast Electrically Tunable Polaritonic Metasurfaces. *Adv. Opt. Mater.* **2**, 1057–1063 (2014).
83. Wan, C. *et al.* On the Optical Properties of Thin-Film Vanadium Dioxide from the Visible to the Far Infrared. *Ann. Phys.* **531**, 1900188 (2019).
84. Zhu, Z., Evans, P. G., Haglund, R. F. & Valentine, J. G. Dynamically Reconfigurable Metadevice Employing Nanostructured Phase-Change Materials. *Nano Lett.* **17**, 4881–4885 (2017).
85. Kang, T. *et al.* Large-scale, power-efficient Au/VO2 active metasurfaces for ultrafast optical modulation. *Nanophotonics* **10**, 909–918 (2020).
86. Kim, H. J., Sohn, J., Hong, N., Williams, C. & Humphreys, W. PCM-net: a refractive index database of chalcogenide phase change materials for tunable nanophotonic device modelling. *J. Phys. Photonics* **3**, 024008 (2021).

87. Zhang, Y. *et al.* Broadband transparent optical phase change materials for high-performance nonvolatile photonics. *Nat. Commun.* **10**, 4279 (2019).
88. Meng, J. *et al.* Electrical Programmable Low-loss high cyclable Nonvolatile Photonic Random-Access Memory. *arXiv:2203.13337* (2022). doi:10.48550/arxiv.2203.13337
89. Moon, J.-S. *et al.* Reconfigurable infrared spectral imaging with phase change materials. *SPIE Proc.* **10982**, 32 (2019).
90. Greef, R., Kalaji, M. & Peter, L. M. Ellipsometric studies of polyaniline growth and redox cycling. *Faraday Discuss. Chem. Soc.* **88**, 277–289 (1989).
91. Xiong, K. *et al.* Video Speed Switching of Plasmonic Structural Colors with High Contrast and Superior Lifetime. *Adv. Mater.* **33**, 2103217 (2021).
92. Li, Z. *et al.* Correlated Perovskites as a New Platform for Super-Broadband-Tunable Photonics. *Adv. Mater.* **28**, 9117–9125 (2016).
93. Huang, M. *et al.* Voltage-gated optics and plasmonics enabled by solid-state proton pumping. *Nat. Commun.* **10**, 5030 (2019).
94. Li, Y., Van De Groep, J., Talin, A. A. & Brongersma, M. L. Dynamic Tuning of Gap Plasmon Resonances Using a Solid-State Electrochromic Device. *Nano Lett.* **19**, 7988–7995 (2019).
95. Eaves-Rathert, J. *et al.* Dynamic Color Tuning with Electrochemically Actuated TiO2 Metasurfaces. *Nano Lett.* **22**, 1626–1632 (2022).
96. Hopmann, E. & Elezzabi, A. Y. Plasmochromic Nanocavity Dynamic Light Color Switching. *Nano Lett.* **20**, 1876–1882 (2020).
97. Wang, G., Chen, X., Liu, S., Wong, C. & Chu, S. Mechanical Chameleon through Dynamic Real-Time Plasmonic Tuning. *ACS Nano* **10**, 1788–1794 (2016).
98. Palm, K. J., Murray, J. B., Narayan, T. C. & Munday, J. N. Dynamic Optical Properties of Metal Hydrides. *ACS Photonics* **5**, 4677–4686 (2018).
99. Tajima, K., Yamada, Y., Bao, S., Okada, M. & Yoshimura, K. Flexible all-solid-state switchable mirror on plastic sheet. *Appl. Phys. Lett.* **92**, 041912 (2008).
100. Li, J. *et al.* Addressable metasurfaces for dynamic holography and optical information encryption. *Sci. Adv.* **4**, eaar6768 (2018).
101. Yang, W. *et al.* All-dielectric metasurface for high-performance structural color. *Nat. Commun.* **11**, 1864 (2020).
102. Li, J., Yu, P., Zhang, S. & Liu, N. A Reusable Metasurface Template. *Nano Lett.* **20**, 6845–6851 (2020).
103. Hu, J. *et al.* Lattice-Resonance Metalenses for Fully Reconfigurable Imaging. *ACS Nano* **13**, 4613–4620 (2019).
104. Bi, L. *et al.* Magneto-Optical Thin Films for On-Chip Monolithic Integration of Non-Reciprocal Photonic Devices. *Materials* **6**, 5094–5117 (2013).
105. Kazlou, A., Chekhov, A. L., Stognij, A. I., Razdolski, I. & Stupakiewicz, A. Surface Plasmon-Enhanced Photomagnetic Excitation of Spin Dynamics in Au/YIG:Co Magneto-Plasmonic Crystals. *ACS Photonics* **8**, 2197–2202 (2021).
106. Ren, M. *et al.* Nanostructured Plasmonic Medium for Terahertz Bandwidth All-Optical Switching. *Adv. Mater.* **23**, 5540–5544 (2011).
107. Shcherbakov, M. R. *et al.* Ultrafast all-optical tuning of direct-gap semiconductor metasurfaces. *Nat. Commun.* **8**, 17 (2017).
108. Wu, Y., Kang, L., Bao, H. & Werner, D. H. Exploiting Topological Properties of Mie-Resonance-Based Hybrid Metasurfaces for Ultrafast Switching of Light Polarization. *ACS*

Photonics **7**, 2362–2373 (2020).

Acknowledgments

This work was sponsored by the National Science Foundation under award number 2132929, Defense Advanced Research Projects Agency Defense Sciences Office Program: EXTREME Optics and Imaging (EXTREME) under agreement number HR00111720029, the National Institute of Aerospace, and Lockheed Martin Corporation Internal Research and Development. The authors would like to thank Sensong An and William Humphreys for creation of graphics, Fan Yang and Xiaoming Qiu for assistance with optical/thermal modelling, as well as Matthew Julian, Calum Williams, Xiaochen Sun, Xu Fang, and Lei Bi for helpful technical discussions and assistance with development of the outline. The views, opinions and/or findings expressed are those of the authors and should not be interpreted as representing the official views or policies of the Department of Defense or the U.S. Government.

Author contributions

All authors contributed to writing the paper.

Materials & Correspondence

Correspondence and requests for materials should be addressed to Juejun Hu.

Competing financial interests

The authors declare no competing interests.